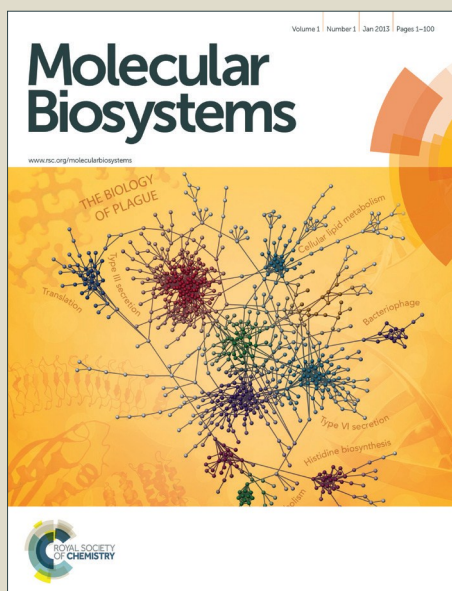


Molecular BioSystems

Accepted Manuscript



This is an *Accepted Manuscript*, which has been through the Royal Society of Chemistry peer review process and has been accepted for publication.

Accepted Manuscripts are published online shortly after acceptance, before technical editing, formatting and proof reading. Using this free service, authors can make their results available to the community, in citable form, before we publish the edited article. We will replace this *Accepted Manuscript* with the edited and formatted *Advance Article* as soon as it is available.

You can find more information about *Accepted Manuscripts* in the [Information for Authors](#).

Please note that technical editing may introduce minor changes to the text and/or graphics, which may alter content. The journal's standard [Terms & Conditions](#) and the [Ethical guidelines](#) still apply. In no event shall the Royal Society of Chemistry be held responsible for any errors or omissions in this *Accepted Manuscript* or any consequences arising from the use of any information it contains.



www.rsc.org/molecularbiosystems



Journal Name

ARTICLE

Received 00th January 20xx,
Accepted 00th January 20xx
DOI: 10.1039/x0xx00000x

www.rsc.org/

Reconstruction and analysis of a genome-scale metabolic model for *Eriocheir sinensis* eyestalk

Bin Wang,^{a,b} Qianji Ning,^{*a} Tong Hao,^{*b} Ailing Yu,^b and Jinsheng Sun^{*b}

Eyestalk of *Eriocheir sinensis* have significant biological functions with many nerve peptide hormones expressed in X-organ which exists in eyestalk. Metabolic network model is an effective tool for the systematic study of *E. sinensis* eyestalk. In this work, we reconstructed a metabolic network model for *E. sinensis* eyestalk based on the transcriptome sequencing. The model contains 1304 reactions, 1381 unigenes and 1243 metabolites distributing in 98 pathways. The reconstructed metabolic network model was used for functional module and block metabolites analysis of eyestalk, which reveals that the function of the eyestalk network is agree with its function as the centre of the *E. sinensis* endocrine system. The difference expression analysis of reactions in the model indicates that the eyestalk mainly functions in the regulation of amino acids, carbohydrate and nucleotide metabolism.

Introduction

E. sinensis, also known as crab, is one of the most important aquatic economic animals with high commercial value as a food source. Many studies has been performed focusing on several or single genes¹, proteins² or a specific pathway³ to accelerate the growth or further investigating the metabolic system of *E. sinensis*. In 2014, Sun Yan et al conducted transcriptome sequencing on the hepatopancreas, eyestalk and Y-organ of *E. sinensis*⁴. Subsequently, Hao Tong et al constructed the protein interaction network of these organs⁵. Eyestalk which contains the X-organ sinus gland (XO-SG) is known as the endocrine control center of *E. sinensis*. It secretes and produces a variety of neuropeptide hormones which regulate important physiological activities of the crustacean animals, such as growth, metabolism and reproduction.

Many researches have focused on the profiles or genes of eyestalk^{6,7}. However, a systematic study of eyestalk metabolic system is still missing. In recent decades, a front trend of the network biology is to use genomic data and molecular mechanisms to construct predictive models⁸. Genome-scale metabolic network model is an important part in this area and supplies a useful tool for the system study of specific organisms or organ⁹. In recent years, with the development of high throughput data analysis, the reconstruction of genome-scale metabolic network model has developed rapidly^{10,11} with interaction of knowledge on biochemistry and physiological metabolism¹². Since Edwards and Palsson et al constructed the

first genome-scale of metabolic network model for *Haemophilus influenzae* in 1999¹³, plenty of models have been constructed and applied in the analysis of various biological phenotype, which reflects the important role of genome-scale metabolic network model for the research of metabolism in a wide range of organisms. Currently, more than one hundred metabolic network models have been reconstructed for bacterial¹⁴, plants^{15,16}, animals¹⁷ and human^{18,19}. The models have a widely use to areas such as metabolic engineering, antibiotic design, and organismal and enzyme evolution.²⁰

For the systematic study for the metabolic function of *E. sinensis* eyestalk, we reconstructed a genome-scale metabolic model for eyestalk based on the transcriptome sequencing. The model was revised with the simulation on the synthesis capability of non-essential amino acids. Function analysis of the reconstructed model was used to reveal the fundamental function of eyestalk metabolism system and the vital function as the center of the crustaceans endocrine system. The differentially expressed unigenes were analyzed to further understanding the influence of 5-HT and glucose on the metabolism of eyestalk. The model provides a useful tool for the in-depth study on the function of *E. sinensis* eyestalk, as well as provides an important reference for future study of aquatic crustacean species.

Methods

Preliminary reconstruction of genome-scale metabolic network model

The unigene information was obtained from the transcriptional sequencing of *E. sinensis* eyestalk⁴. The KO annotated of the unigenes was supplied in the work of Yan Sun et al⁴. The related biochemical information of proteins, metabolic reactions, pathways and metabolic subsystems was matched from KEGG database with KO as a bridge. The draft reconstruction is obtained with the relationship of unigene-protein-reaction is established according to the KEGG database.

^a College of Life Sciences, Henan Normal University, Xinxiang 453007, Henan, P.R. China.

E-mail: nqjnqj1964@163.com

^b Tianjin Key Laboratory of Animal and Plant Resistance/College of Life Science, Tianjin Normal University, Tianjin 300387, P.R. China.

E-mail: jinshsun@163.com

Electronic Supplementary Information (ESI) available: [details of any supplementary information available should be included here]. See DOI: 10.1039/x0xx00000x

The draft reconstructed metabolic network on the genome-scale is far from perfect. Further curation is needed. Firstly, the chiral molecule of glucose is revised. In KEGG database, glucose was shown in three forms: D-glucose, alpha-D-glucose and beta-D-glucose. D-glucose is the general name of glucose, which includes both alpha-D-glucose and beta-D-glucose. In order to avoid the confusion of glucose in the following curation and simulation, all the glucose in the network was unified to be alpha-D-glucose as alpha type is the main existing form of most sugar in biological organisms.

Gap filling

The gaps in the network was filled with the method based on the connectivity of weak connected components (WCCs)^{21, 22}. Firstly, the reactions that exist in the whole reaction list from KEGG database but not the preliminary reconstructed network was considered as the candidate dataset for gap filling. Secondly, as graph theory has been proved to be a useful train of thought for biological analysis²³⁻²⁶, the network was converted into a reaction map with reactions as nodes and metabolites as edges according to the metabolic flux direction. In this way, the metabolic network was divided into different WCCs. Finally, the reactions that could be used to connect different WCCs were searched in the candidate dataset. These reactions were identified as the gap filling reactions.

The gaps were filled both on the pathway²¹ and global scale²². These two methods were used sequentially to fill the gaps in the network to a maximum extent. Gap filling on the pathway scale prefers to decrease the number of WCCs in the same pathway, whereas that on the global scale inclines to reduce the WCCs in the whole network.

Simulative curation of the model

In order to determine whether the reconstruction can correctly reflect the metabolic processes of the living organisms, we firstly convert the reaction list to standard SBML document which can be read by COBRA²⁷ and analyzed with flux balance analysis (FBA) which is the commonly used optimization simulation methods²⁸⁻³⁰ for metabolic networks.

The flux ranges of reactions in the network were limited for simulation. The upper and lower flux of the reversible reaction, the irreversible reaction and the transport reaction were set to be (-1000, 1000)¹² (0, 1000), and (-1000, 1000) mmol g DW⁻¹ h⁻¹, respectively. The limits of exchange reactions for essential amino acids, glucose, H₂O, Fe³⁺, alpha-D-Glucose, Potassium, Magnesium, Calcium, which are needed to be exchanged with the environment were set to (-5, 1000) mmol g DW⁻¹ h⁻¹, while those for non-essential amino acids which can be synthesized by *E. sinensis* were set to (0, 1000) mmol g DW⁻¹ h⁻¹.

In order to investigate the biosynthesis capability of non-essential amino acids (alanine, asparagine, aspartic acid, cysteine, glutamine, glutamate, glycine, proline, serine, and tyrosine), 10 non-essential amino acids were set to be objective functions, respectively. If an amino acid cannot be synthesized, there must be absence of reaction(s) in the network. The missing reaction(s) are found by backtracking along the synthesis pathway of the amino acid. With the addition of missing reaction(s), the production of the amino

acid was calculated again to confirm the synthesis capability of the model.

Network decomposition

Model decomposition is performed by applying the method based on the combination of dendrogram and modularity^{31, 32}. The network was decomposed with four steps. Firstly, the network was converted into a reaction map. In order to achieve the conversion, current metabolites (such as ATP, ADP, H₂O, NAD⁺, NADH, Pi³³) are firstly removed. Reactions exist as nodes and the metabolites act as edges in the map. Secondly, the reaction map was preliminary decomposed according to the dendrogram tree with no more than 50 nodes in a cluster. Thirdly, the preliminary decomposition was optimized by elimination of Very Small Cluster (VSC) with no more than 10 nodes as the first optimization step. Fourthly, the modularity of the network was maximization in the second optimization step with the final number of cluster set to be 10. With the decrease of module numbers in the fourth step, the partition with highest modularity was considered as the final decomposition result.

Detection of differentially expressed protein in eyestalk

The healthy *E. sinensis* (body weight 5-6g), with good vitality were bought from Huada, and then acclimatized in freshwater at 18-20°C for 3-5 days.

A total of 180 *E. sinensis* that were selected randomly from the rearing animals in the laboratory were equally divided into three groups. The group that were injected with 5-HT was the experimental group (A1). The second group that were injected with glucose was the experimental group (A2). The third group, which were injected with distilled water, was the control group (A0). (The weight of each *E. sinensis* was measured before injection. The volume injected (ul) was the same as the weight (g) in terms of number). One hour later, eyestalks of *E. sinensis* from all these groups were removed and frozen in liquid nitrogen immediately storing at -80°C until extraction of RNA.

To extract RNA, the following steps were taken. Firstly, the total RNA from eyestalk in group A0, A1 and A2 was extracted using the TRIzol method (Invitrogen, USA). Secondly, the cDNA was synthesized using the superScript III first-strand synthesis system (Invitrogen, USA). After extracting the total RNA from the three samples, the generated cDNA library was sequenced using Illumina HiSeqTM2000.

Results and discussion

Preliminary reconstruction of the network

Totally 48835 unigenes were obtained in the transcriptional sequencing of eyestalk, in which 12864 were found to be matched with KO from KEGG database⁴. The preliminarily reconstructed metabolic network was obtained through matching unigenes to related reactions and pathways from KEGG database through KO as a bridge. The network included 1208 reactions and 1381 unigenes, which distributed in 98 pathways and 11 subsystems (additional file 1). 6 reactions with D-glucose were curated to be alpha-D-glucose for the standardization of chiral metabolites.

Gap filling

A 'gap' is defined as a reaction that takes place in a pathway/network different to that of its two neighbor reactions. Network gaps will lead to unbalanced flux distribution. Therefore, it is necessary to fill them before simulation. Filling gaps can improve the connectivity of the network and enable a pathways to perform its normal function³⁴.

Gaps were filled on the pathway and global scale sequentially. With gap filling in the pathway scale, the number of reactions in the network increased from 1028 to 1186. 158 new reactions were added, most of which were involved in metabolism of arginine, proline, caffeine, cysteine, methionine, sphingolipid, cytochrome P450 and biosynthesis of phenylpropanoid and steroid. With gap filling in the global scale, 60 more reactions were added. The number of WCCs decreased from 218 to 79 in the gap filling step, in which 108 decreases in the pathway scale and 31 decreases in the global scale. After gap filling, the network contains 1246 reactions.

Addition of transport and exchange reactions

In order to distinguish the intracellular and extracellular parts of the cell, the metabolites and reactions in the network were divided into two compartments: intracellular and extracellular. The metabolites were discriminated as intracellular or extracellular according to their locations. The reactions with all the related metabolites located in intracellular are identified as intracellular reactions. The reactions with all the related metabolites in extracellular are identified as extracellular reactions. The reactions with related metabolites distribute in both intracellular and extracellular are identified as transport reactions.

Actually most reactions in the metabolic network are intracellular reactions, whereas the organisms cannot grow without exchanging substances with extracellular environment by absorbing nutrients or discharging metabolic products. In order to enable the model the capability of exchanging substances with the outside world, transport and exchange reactions for the basic nutrients that the eyestalk cells may exchange with external environment were added. We totally added transport and exchange reactions for 26 substances including 20 kinds of amino acids, H₂O, Fe³⁺, Potassium, alpha-D-Glucose, Magnesium and Calcium. With addition of transport and exchange reactions, 1299 reactions were included in the network. Both intracellular and extracellular metabolites are involved in the transport reactions, and all the metabolites are in extracellular in the exchange reactions.

Simulation curation

In order to investigate the quality of the model, the capability of synthesizing non-essential amino acids were verified. The result showed that two of non-essential amino acids, asparagine and cysteine, cannot be synthesized. According to the map of Alanine, aspartate and glutamate metabolism in KEGG, L-Asparagine (KEGG NO.: C00152) is the product of two reactions (R00483 and R00578). When R00483 (ATP + L-Aspartate + Ammonia \rightleftharpoons AMP + Diphosphate + L-Asparagine) is added to the network,

asparagine can be successfully synthesized. Therefore, it was finally found that the break of asparagines synthesis route is due to the absent of reaction R00483. With the same way, the synthesis route of cysteine (C00097) was remedied by the addition of four reactions (R00528, R00858, T00027, E00027). These reactions enable the network to absorb sulfate from environment³⁵ and convert it into sulfide which is necessary in the synthesis of cysteine. With these curations, all the ten non-essential amino acids can be successfully synthesized by the reconstructed network model. The curated model contains 1340 reactions, 1243 metabolites, 1381 unigenes, which distributes in 98 pathways and 11 subsystems (supplementary file 1). The overview characteristics of the reconstructed model are shown in Table 1.

Table 1 The characteristics of genome-scale metabolic network model of eyestalk

Items	Count
Unigenes	1381
Reactions	1304
Metabolic reactions	1250
Transport reactions	27
Exchange reactions	27
Metabolites	1243
Intracellular metabolites	1214
Extracellular metabolites	29
Pathways	98
Subsystems	11

Topology and function analysis of reconstructed metabolic network model

Topology analysis

The genome-scale metabolic model for *E. sinensis* eyestalk was composed of 1304 reactions. Its topological features, which were calculated with Pajek software³⁶ were shown in Table 2. Besides the exchange reactions, there were 1277 reactions in the network. After removing of currency metabolites, 1246 main reactions are extracted, in which 1128 are non-isolated reactions. Therefore, the reaction map of the network, which was composed of the non-isolated reactions, contains 1128 reactions. The network has the bow-tie structure, which is in consistent with the conclusion made by Zhao Jing et al³⁷ that bow-tie structure is widespread in the metabolic network in different levels, sizes, chemical and spatial unit. The metabolic network was divided into 71 WCCs which include nine bigger WCCs that contains more than 10 reactions. The biggest one included 797 reactions, which takes up about 70.66% of the total number of reactions in the metabolic network (as shown in Fig. 1). In order to further analysis the function of the metabolic network, the biggest weak component was decomposed with the method described in the Method section. After two times of optimization in the decomposed process, the connection within modules increased gradually, while that between modules gradually reduced. The network modularity increased (as shown in Table 3), which indicates that the modularity of the metabolic network was gradually strengthened. When the number of the modules decreased to 16 we got the highest

modularity value 0.827. Therefore, the 16 modules were taken as the final decomposition result (supplementary file 2).

Table 2 The basic topological features of the reconstructed metabolic network

graph metrics		value
Nodes		1128
	arcs	1970
	edges	769
Density		0.002757
average degree		4.856383
average path length		8.95101
Diameter		21
biggest cluster	nodes	797
	arcs	1702
	edges	717
bowtie of biggest cluster	GSC	394(49.4%)
	S	75(9.4%)
	P	253(31.7%)
	IS	75(9.4%)

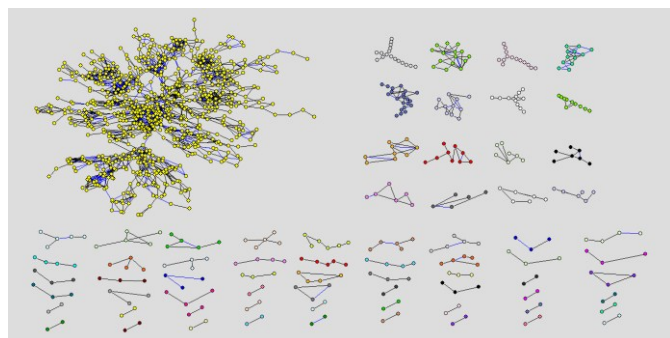


Fig. 1 The WCCs (weak connected components) in the eyestalk metabolic network. Totally 71 components are shown which are distinguished by different colors.

Table 3 Decomposition result of the eyestalk metabolic network

	Threshold	Modules	Modularity
priliminary	50	57	0.622
First	10	22	0.812
Second	10	16	0.827

Function analysis

In order to further understand the metabolic function of eyestalk, the main function of each module in the biggest weak component was further analyzed. Its main functions include basic amino acid metabolism, carbohydrate metabolism, nucleic acid metabolism and lipid metabolism (Fig. 2). Most of the modules were dominated by one or two kinds of subsystems suggesting that the function of each module was relatively independent. The amino acid metabolism dominated in the metabolic network of eyestalk (Table 4). Amino acid is the basic substance in the synthesis of neuropeptide hormones. Therefore, the function of the modules is in consistent with the fact that X-organ sinus gland (XO-SG) secretes neuropeptide hormones, which is the main function of eyestalk³⁸. In addition, carbohydrate metabolism

also takes up a large proportion in the network because of its close relationship with other metabolisms, which indicating that eyestalk may also play a role in the energy offering and converting process. The fact that different metabolic pathways are contained in one module shows that one metabolic function may be accomplished through several pathways. For example, aspartic acid in module 14 can be converted to arginine; module 9 includes the metabolism of folic acid and purine, which coincides with one of the functions of folic acid: involvement in the biosynthesis of purine ring and deoxynucleotide³⁹, module 14 includes the metabolism of folic acid and glutamic acid. Folic acid, also known as pteroylglutamic acid, is involved in the biosynthesis of glutamic acid and the metabolism of arginine⁴⁰ (some scholars regards that folic acid in the body exists in two forms: transport folic acid is in the form of mono-glutamic acid, storage folic acid is in the form of poly-glutamic acid⁴¹).

To further confirm the core function of the modules, we considered the reactions with the highest degree in the module as the core reactions and analyzed the subsystem of the core reactions, which may inflect the core function of the related module. The first three reactions with the highest degrees were checked. We found that the function of the core reactions in each module agreed well with the main functions in fig. 2 (supplementary file 3).

In the common metabolism process of a cell, exogenous nutrients are firstly decomposed into primary metabolites and then synthesized into 12 kinds of common precursors, such as glucose-6-phosphate, fructose-6-phosphate, phosphoenolpyruvic acid, pyruvic acid (as shown in Fig. 3). The common precursors are subsequently used for the synthesis of the key components of the cell, such as amino acids, nucleotides, fatty acid and sugar⁴². In order to verify the basic metabolic functions of genome-scale metabolic network model for *E. sinensis* eyestalk, the synthesis process of the 12 common precursors were investigated. As shown in Fig. 3, all the 12 precursors can be found in the network. They distributes in three modules, and half of them were in module 12 where reactions were mainly associated with carbohydrate metabolism. The TCA cycle scattered in two modules, which agreed with the diversity of the TCA pathway⁴³. In addition to the common precursors, module 16 contained a number of building blocks from these precursors, such as aspartate and asparagine. The above analysis showed that eyestalk has the basic capability of synthesizing common precursors and building blocks.

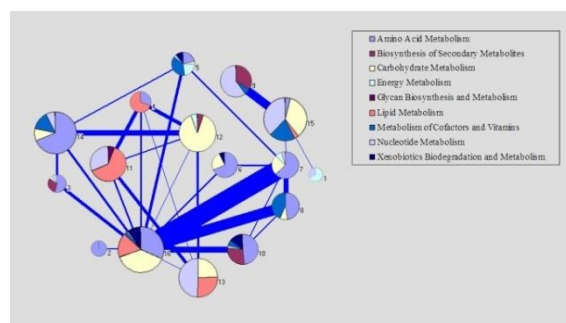


Fig. 2 Function analysis of the reconstructed metabolic network. Each pie chart represents a single module which divided into several different subsystems. The percentage of reactions in a certain subsystem are shown by the area in a pie chart. The thickness of the line between modules represents the strength of the connection.

Table 4 Distribution of amino acid metabolism in modules

Module number	Metabolic process
Module 2	Lysine biosynthesis and degradation
Module 3	Leucine and isoleucine degradation
Module 4	Glycine metabolism
Module 5	Tryptophan metabolism
Module 6	Isoleucine degradation
Module 7	Serine and glycine metabolism
Module 8	Cysteine metabolism
Module 10	Tyrosine and phenylalanine metabolism
Module 14	Arginine, proline, glutamate metabolism
Module 15	Cysteine metabolism
Module 16	Lysine, isoleucine degradation; glycine metabolism

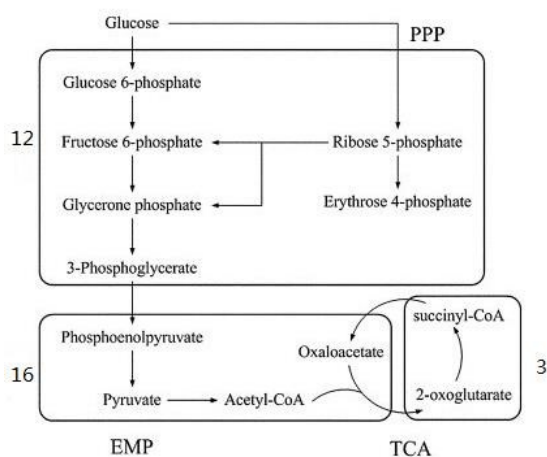


Fig. 3 Distribution of 12 precursors in the modules of eyestalk metabolic network. All precursors were distributed in three modules, and half of them centered in module 12

Analysis of differentially expressed unigenes

In the comparison of the mRNA expression from A0 with that from A1 and A2, we got 51810 and 53833 differentially expressed unigenes respectively. In these unigenes, both 135 can be found in the metabolic network respectively (supplementary file 4). The result of expression profile is shown in Table 5.

Table 5 The results of the experiment

Experimental	Differentially expressed unigenes	Differentially expressed unigenes in module	Differentially expressed unigenes in the biggest WCC

A0	51810	Up	12716	135	Up	11	89	Up	5
A1		Down	39094		Down	124		Down	84
A0	53833	Up	49048	135	Up	118	89	Up	77
A2		Down	4785		Down	17		Down	12

5-HT injection results in the expression changes of 90 unigenes which are related to 90 reactions. These reactions were mainly in module 7, 11, 12, 13, 14, and 15. To be specific, the metabolic difference reaction of amino acid mostly distributed in module 5 (in which cofactors and vitamins metabolism dominate), module 7, 10, 14 (in which amino acid metabolism dominates) and module 15 (in which nucleotide metabolism and carbohydrate metabolism dominates); the metabolic difference reaction of carbohydrate were in module 15 and module 12 (in which carbohydrate metabolism dominates); the metabolic difference reaction of lipid existed in module 11 and 13 (in which nucleotide metabolism dominates); the metabolic difference reaction of cofactors and vitamin centered in module 3 and 14 (in which amino acid metabolism dominates); the metabolic difference reaction of nucleotide were in module 13 and 15 (as shown in Fig. 4). 5-HT is a neurotransmitter in the nervous system of crustaceans^{44,45}. Its function is to help X organ-sinus gland complex (XO-SG) in the eyestalk of crustaceans to release some neurohormones, such as high blood sugar hormone (CHH)^{46,47}, molt inhibiting hormone (MIH)⁴⁸. The differential expression results shows that the function of 5-HT in eyestalk is accomplished by various metabolic subsystems. The differences between the differentially expressed reactions and the dominated reactions in a module indicate that the injection of 5-HT may influence the dominated metabolisms in the module mainly through the differentially expressed reactions and thereby influence the function of eyestalk.

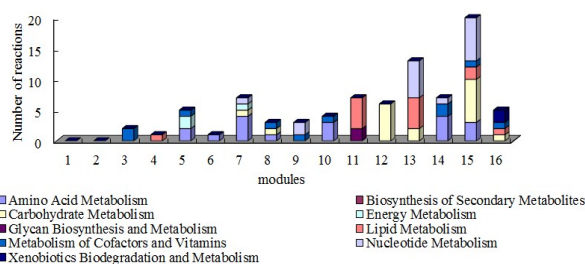


Fig. 4 Function distribution of differentially expressed reactions in the modules of eyestalk network

Differentially expressed genes found after the injection of glucose were the same with those after the injection of 5-HT. It is because that the eyestalk secretes neuropeptides hormone whose chemical nature is protein which was composed by amino acids. Precursors synthesized into amino acid are in the pathways of carbohydrate metabolism. Nucleotide metabolism and amino acid metabolism are closely linked because that they are all related to nitrogen. Lots of the unigenes have different change trends after injection of glucose and 5-HT.

The main metabolic processes influenced by these unigenes were shown in Table 6. That may be because that the injection of 5-HT motivates the release of CHH which improves the increase of blood sugar, whereas the injection of glucose may inspire the regulation for decreasing the blood sugar. 5-HT/glucose exert an effect on the metabolism of several substances in eyestalk, such as ammonia acid, proline, amino sugars and uracil, thus affecting the metabolic process of *E. sinensis*.

Table 6 The different influence on metabolic process between injection of 5-HT and glucose

Pathway		Process	General trend	
			5-HT	Glucose
Amino acid metabolism	Arginine and proline metabolism	L-Arginine→L-Arginine phosphate; L-Proline→Hydroxyproline	Down	Up
	Glycine, serine and threonine metabolism	Sarcosine↔Glycine↔L-Threonine; Serine ↔ L-Cysteine	Down	Up
	Cysteine and methionine metabolism	AdoMet→S-Adenosylhomocysteine→Homocysteine	Down	Up
Carbohydrate metabolism	Pentose phosphate pathway	beta-D-Fructose 6-phosphate →alpha-D-Glucose 6-phosphate	Down	Up
	Amino sugar, nucleotide sugar metabolism	GlcNAC→GlcNAC-6P→GlcNAC-1P→UDP-GlcNAC→ Chitin	Down	Up
Nucleotide metabolism	Uracil metabolism	UDP↔UMP↔Uracil↔Pseudouridine 5'-phosphate	Down	Up
	Adenine metabolism	GMP → IMP ← AMP ↔ ADP ↕ Hypoxanthine	Down	Up
Lipid metabolism	Sphingolipid metabolism	Dihydroceramide→Ceramide↔Sphingomyelin	Down	Up
	Glycerophospholipid metabolism	Ethanolamine→Ethanolamine phosphate→CDP-ethanolamine	Down	Up

Conclusions

Genome-scale metabolic network model has been widely used in the analysis of the metabolic function and processes for many kinds of organisms. In this work, we reconstructed a genome-scale metabolic network for *E. sinensis* eyestalk on the basis of transcriptome sequencing. The biological feature of the model was evaluated by the topology analysis. The analysis of the biggest WCC shows that amino acid metabolism and carbohydrate metabolism constitute the largest proportions in the eyestalk which indicate the function of eyestalk in peptide hormones section and energy metabolism. 5-HT and glucose injections lead to the changes in amino acid metabolism and carbohydrate metabolism, which illustrates that 5-HT and glucose may influence the

neuropeptide hormone secretion of the eyestalk, and further certified that eyestalk is the control center of the endocrine system in *E. sinensis*.

Acknowledgements

This work was supported by National High-Tech Research and Development Program of China (863 programs, 2012AA10A401), Grants of the Major State Basic Research Development Program of China (973 programs, 2012CB114405), National Key Technology R&D Program (2011BAD13B07 and 2011BAD13B04), National Natural Science Foundation of China (21106095, 61100124), Natural Science Foundation of Tianjin (15JCYBJC30700), Foundation of Introducing Talents to Tianjin Normal University (5KQM110003), Academic innovation promotion project of Tianjin Normal University for young teachers(52XC1403), and “131” Innovative Talents cultivation of Tianjin.

Notes and references

- A. Q. Yu, X. K. Jin, X. N. Guo, L. Shuang, M. H. Wu, W. W. Li and Q. Wang, *Fish & Shellfish Immunology*, 2013, **35**, 1282-1292.
- Y. Wang, Y. Zhang, Y. Sun, Y. Liu, X. Geng and J. Sun, *Journal of Fisheries of China*, 2013, **37**, 987-993.
- X. Li, Z. Cui, Y. Liu, C. Song and G. Shi, *PLoS one*, 2013, **8**, 374-374.
- Y. Sun, Y. Zhang, Y. Liu, S. Xue, X. Geng, T. Hao and J. Sun, *PLoS one*, 2014, **9**, e95827.
- H. Tong, Z. Zheng, B. Wang, Y. Zhang, Y. Liu, X. Geng and J. Sun, *Bmc Systems Biology*, 2014, **8**, 417-422.
- G. Zhengbing, Y. Shui, X. Zhou, X. Zenghong and Z. Zhao, *Jiang Su Agricultural Sciences*, 2012, **40**, 28-30.
- P. S. Sun, *Molecular Marine Biology & Biotechnology*, 1995, **4**, 262-268.
- E. Wang, N. Zaman, S. Mcgee, J. S. Milanese, A. Masoudi-Nejad and M. O'Connor-Mccourt, *Seminars in Cancer Biology*, 2015, **30**, 4-12.
- J. D. Orth, T. M. Conrad, J. Na, J. A. Lerman, H. Nam, A. M. Feist and B. Ø. Palsson, *Molecular systems biology*, 2011, **7**, 535.
- R. A. Notebaart, F. H. V. Enckevort, C. Francke, R. J. Siezen and B. Teusink, *Bmc Bioinformatics*, 2006, **7**, : 296.
- C. Francke, R. J. Siezen and B. Teusink, *Trends in Microbiology*, 2005, **13**, 550-558.
- I. Thiele and B. Ø. Palsson, *Nature protocols*, 2010, **5**, 93-121.
- J. S. Edwards and B. O. Palsson, *Journal of Biological Chemistry*, 1999, **274**, 17410-17416.
- T. Hao, B. Han, H. Ma, J. Fu, H. Wang, Z. Wang, B. Tang, T. Chen and X. Zhao, *Molecular bioSystems*, 2013, **9**, 2034-2044.
- R. Saha, P. F. Suthers and C. D. Maranas, *PLoS one*, 2011, **6**, e21784-e21784.
- S. Mintz-Oron, S. Meir, S. Malitsky, E. Ruppin, A. Aharoni and T. Shlomi, *Proc. Natl. Acad. Sci. U.S.A.*, 2012, **109**, 339-344.
- M. Sigurdsson, N. Jamshidi, E. Steingrimsson, I. Thiele and B. Palsson, *BMC Syst Biol*, 2010, **4**, 140.
- H. Ma, A. Sorokin, A. Mazein, A. Selkov, E. Selkov, O. Demin and I. Goryanin, *Mol. Syst. Biol.*, 2007, **3**, 135.

19. N. Duarte, S. Becker, N. Jamshidi, I. Thiele, M. Mo, T. Vo, R. Srivas and B. Palsson, *Proc. Natl. Acad. Sci. U.S.A.*, 2007, **104**, 1777-1782.
20. E. O'Brien, J. Monk and B. Palsson, *Cell*, 2015, **161**, 971-987.
21. T. Hao, H.-W. Ma, X.-M. Zhao and I. Goryanin, *BMC bioinformatics*, 2010, **11**, 393.
22. T. Hao, H.-W. Ma, X.-M. Zhao and I. Goryanin, *Molecular bioSystems*, 2012, **8**, 663-670.
23. A. Liu, Z. Wang, W. Nie and Y. Su, *Information Sciences*, 2015, **320**, 429-442.
24. A. A. Liu, K. Li and T. Kanade, *IEEE Transactions on Medical Imaging*, 2012, **31**, 359 - 369.
25. A. A. Liu, Y. T. Su, P. P. Jia, Z. Gao, T. Hao and Z. X. Yang, *IEEE Transactions on Cybernetics*, 2015, **45**, 1194-1208.
26. A. A. Liu, Y. T. Su, W. Z. Nie and Z. X. Yang, *PloS one*, 2015, **10**.
27. S. A. Becker, A. M. Feist, M. L. Mo, G. Hannum, B. Ø. Palsson and M. J. Herrgard, *Nature protocols*, 2007, **2**, 727-738.
28. J. M. Lee, E. P. Gianchandani and J. A. Papin, *Briefings in bioinformatics*, 2006, **7**, 140-150.
29. J. M. Park, T. Y. Kim and S. Y. Lee, *Biotechnology advances*, 2009, **27**, 979-988.
30. D. Koschützki, B. H. Junker, J. Schwender and F. Schreiber, *Journal of theoretical biology*, 2010, **265**, 261-269.
31. H. W. Ma, X. M. Zhao, Y. J. Yuan and A. P. Zeng, *Bioinformatics*, 2004, **20**, 1870-1876.
32. T. Hao, B. Wang, A. Yu, A. Liu and J. Sun, *MNetDec: A Flexible Algorithm for Metabolic Network Decomposition*, 2015.
33. H. Ma and A.-P. Zeng, *Bioinformatics*, 2003, **19**, 270-277.
34. R. L. Chang, L. Ghamsari, A. Manichaikul, E. F. Hom, S. Balaji, W. Fu, Y. Shen, T. Hao, B. Ø. Palsson and K. Salehi - Ashtiani, *Molecular systems biology*, 2011, **7**, 518.
35. J. M. Dreyfuss, J. D. Zucker, H. M. Hood, L. R. Ocasio, M. S. Sachs and J. E. Galagan, *PLoS Comput Biol*, 2013, **9**, e1003126.
36. V. Batagelj and A. Mrvar, *Connections*, 2008.
37. J. Zhao, H. Yu, J.-H. Luo, Z.-W. Cao and Y.-X. Li, *BMC bioinformatics*, 2006, **7**, 386.
38. W. Zaizhao and X. Jianhai, *Journal Ournal of Fisheries of China*, 2001, 175-180.
39. J. Dongcai, J. Han, J. Xiaojun and Y. Haiming, *China Feed*, 2014, 29-31+36.
40. K. r. C. Williams, N. E. Renthal, R. D. Gerard and C. R. Mendelson, *Molecular Endocrinology*, 2012, **26**, 1857-1867.
41. J. KAN, L. LI and J.-y. XU, *Chinese Journal of Biochemical Pharmaceutics*, 2009, **4**, 020.
42. M. Csete and J. Doyle, *TRENDS in Biotechnology*, 2004, **22**, 446-450.
43. L. J. Sweetlove, K. F. Beard, A. Nunes-Nesi, A. R. Fernie and R. G. Ratcliffe, *Trends in plant science*, 2010, **15**, 462-470.
44. R. R. Eitenmiller, J. H. Orr and W. W. Wallis, *Chemistry and biochemistry of marine food products*, 1982, 39-50.
45. L. Laxmyr, *Comparative Biochemistry and Physiology Part C: Comparative Pharmacology*, 1984, **77**, 139-143.
46. R. Keller, *Cellular and molecular life sciences*, 1992, **48**, 439-448.
47. W. Lüschen, A. Willig and P. P. Jaros, *Comparative Biochemistry and Physiology Part C: Comparative Pharmacology*, 1993, **105**, 291-296.
48. M. P. Mattson and E. Spaziani, *The Biological Bulletin*, 1985, **169**, 246-255.